Origin of the Reactor Antineutrino Anomalies in Light of a New Summation Model with Parametrized β^- Transitions

A. Letourneau,[1,*] V. Savu,[1] D. Lhuillier,[1] T. Lasserre,[1] T. Materna,[1] G. Mention,[1] X. Mougeot,[2]
A. Onillon,[1,†] L. Perisse,[1] and M. Vivier[1]

[1]*IRFU, CEA, Université Paris-Saclay, 91191 Gif-sur-Yvette, France*
[2]*Université Paris-Saclay, CEA, List, Laboratoire National Henri Becquerel (LNE-LNHB), F-91120 Palaiseau, France*

We investigate the possible origins of the reactor antineutrino anomalies in norm and shape within the framework of a summation model where β^- transitions are simulated by a phenomenological model of Gamow-Teller decay strength. The general trends of divergence from the Huber-Mueller model on the antineutrino side can be reproduced in both norm and shape. From the exact electron-antineutrino correspondence of the summation model, we predict similar distortions in the electron spectra, suggesting that biases on the reference spectra of fission electrons could be the cause of the anomalies.

Reactor antineutrino anomalies are a several-years longstanding problem in neutrino physics. They refer to a $\sim 6\%$ deficit in detection rates, known as the "reactor antineutrino anomaly" (RAA), and a $\sim 10\%$ event excess in the 4–6 MeV range, known as the "5-MeV bump," when comparing experimental data to the state-of-the-art Huber-Mueller (HM) model [1,2]. The RAA was first put in evidence in Ref. [3] by comparison with short baseline reactor experiments, and confirmed by all recent high precision reactor antineutrino experiments [4–7]. The "5-MeV bump" is observed in all the above-cited experiments although with slightly different amplitudes and shapes [8–13].

At present, no consensus has been reached regarding the origins of these anomalies. The RAA was first interpreted as the possibility of the existence of a hypothetical sterile neutrino state, mixing with the active electronic flavor. The best fit parameters for this sterile state to absorb the anomaly are now rejected with high confidence level by several experiments [11,14–17] that tested the sterile neutrino hypothesis in a model-independent way.

On the other hand, the Daya Bay and RENO experiments [18,19] studied the dependence of the antineutrino yield on the fuel composition. They concluded that an $\sim 8\%$ bias in the prediction of the ^{235}U flux could be solely responsible for the RAA. This result is slightly in tension with experiments at research reactors with pure ^{235}U fuel which show a deficit of $(5.0 \pm 1.3)\%$ [7]. Nevertheless, the hypothesis of a normalization bias on ^{235}U spectrum is reinforced by the recent measurement of the ^{235}U to ^{239}Pu electron energy spectra ratio [20] reporting a constant $\sim 5\%$ disagreement with respect to the HM prediction.

Regarding the shape anomaly, extensive studies [21–26] have been conducted to find explanations in the prediction modeling, but none of them have succeeded to bring a general consensus in the community.

The Huber-Mueller model is based on an improved method for converting cumulative β^- spectra measured at Institut Laue-Langevin (ILL) with a magnetic spectrometer called BILL [27–29] to antineutrino spectra. With this method, all experimental biases, if they exist, are automatically transferred to the converted antineutrino spectra and may be the cause of the anomalies.

This Letter uses the exact electron-antineutrino correspondence of a refined summation model (SM) to detect any bias in the reference β spectra. The originality of the study lies in the modeling of missing transitions with a new phenomenological β-strength model. The potential biases associated to those transitions are discussed.

The summation method consists of modeling the electron and antineutrino energy spectra at the level of a single β transition and to sum over all the transitions for all the decaying fission fragments. Thus, the electron and antineutrino spectra are calculated in the same theoretical framework, using the same inputs and preserving the symmetry of the two-lepton spectra at the single-branch level. The cumulative energy spectrum for electrons and antineutrinos produced in a reactor is given by

$$S(E,t) = \sum_f A_f(t) \sum_b I_b \times S_f^b(E) \qquad (1)$$

where the f index runs over all fission fragments, and the b index runs over all β branches for a fission fragment.

The time-dependent term $A_f(t)$ is the β^--activity of the fragment after a time t of irradiation. We used the FISPACT-II code [30] with the JEFF3.3 [31] independent fission yields as input to compute the activities after the short irradiation times used for the reference ILL measurements. Although most nuclei have their decay in equilibrium with their production after 12 hours of irradiation, this approach allows for the remaining nuclei that are not yet in equilibrium to be calculated with the correct activities. Because the covariance matrices are not available in JEFF3.3, we used the renormalized covariance matrices for cumulative fission yields from Matthews et al. [32] to estimate the uncertainties on the activities. These matrices encapsulate the uncertainties on the decay of the fission fragments and are good approximations even if not all nuclei are in equilibrium.

The energy dependent term $S_f^b(E)$ is the energy spectrum of electrons or antineutrinos corresponding to a transition. We used the BESTIOLE code developed in Ref. [2] and recently updated in Ref. [33] to calculate this term. It encompasses the most advanced derivations of the first principles of Fermi's theory with finite size and weak magnetism corrections. For simplicity and to highlight the effect of missing transitions, we consider in this Letter only allowed transitions. The effect of first forbidden transitions is discussed later in the text.

Finally, the I_b term is the intensity of the transition to an excited state (E_j) of the daughter nucleus (Z, A). In this Letter, I_b is derived from a Gamow-Teller strength model [$B_{GT}(E_j)$] that will be detailed later, using the following equation:

$$I_b(E_j) = D f(E_j) T_{1/2} B_{GT}(E_j). \tag{2}$$

D is a constant to ensure the right unit to the strength. $T_{1/2}$ is the half-live period of the nucleus. The phase-space integral $f(E_j)$ for allowed transitions is calculated as

$$f(E_j) = \int_0^{E_0} \mathcal{F}(Z, A, E_j) p_e (E + m_e c^2)(E_0 - E)^2 dE \tag{3}$$

with $E_0 = Q_\beta - E_j$ the energy available in the transition (Q_β, the total β-decay energy, is taken from NUBASE [34]), $\mathcal{F}(Z, A, E_j)$ the usual Fermi function for the daughter nucleus, and p_e and E the lepton momentum and kinetic energy, respectively. Fermi transitions are neglected in this Letter because their strength is contained within a very narrow resonance located above the β^--decay window for most of the fission fragments.

The SM fully relies on the available data or models for the fission yields and for the β decay. As stated in previous studies [2,23,24,35,36], it suffers from the uncertainties or lack of data in the databases. Whereas fission yields for the two major actinides ^{235}U and ^{239}Pu are quite well known, the situation is different for β-decay data. The evaluated

nuclear structure data file (ENSDF) β^--decay database [37] suffers from a lack of knowledge for the more unstable isotopes, and when they are known, some transition intensities are affected by the pandemonium effect [38]. It results in an underestimation of the total number of electrons and antineutrinos per fission and an overestimation of the high-energy part of the reconstructed energy spectra [2]. To circumvent this problem, the most sophisticated summation model [35,36] integrates experimental data from calorimetric measurements and the Gross theory to complete the database at high excitation energy. Unfortunately, the calorimetric measurements do not cover all the fission fragments that need to be corrected, and the problem of missing transitions may still persist to some extent.

To overcome this problem, we have developed a β-decay strength model to generate missing transitions for all fission fragments. As explained previously, only Gamow-Teller (G-T) transitions are considered. The G-T model is based on an exhaustive analysis of the experimental strength functions extracted from the low-resolution total absorption gamma spectrometry (TAGS) measurements [39–44] using Eq. (2) (see Ref. [45] for more details on the model). The 66 nuclei, from ^{84}Br to ^{158}Eu, present in the dataset are considered to be representative of β decays of fission fragments. From these data, we derived a universal feature for the β strength as a function of the excitation energy: a discrete domain at low energy and a continuous domain, with a resonance structure, at higher energy.

In our model, the data for the discrete transitions (energy levels and relative beta feedings) are taken from the ENSDF beta-decay database, in priority. When no data exists (for about 3.5% of the total fission fragments activity for ^{235}U), discrete transitions are randomly generated with a simple model that uses level densities to draw fictitious level schemes and imposes that the intensities are normalized to one.

In both cases, the continuous domain is filled with random resonances whose properties (spacing, width, and amplitude) are extracted from the TAGS strength. The resonance spacings vary between 0.1 and 1 MeV with a mean spacing centered around 340 keV. The resonance widths depend slightly on the excitation energy and vary between 20 and 100 keV. The resonance amplitudes are contained within an envelope for which the upper limit follows the trend of the nuclear level density. To calculate this upper limit for each nucleus, we used the nuclear level densities [$\rho_{HFB}(E_{exc}, Z, A)$] from RIPL3 [46], calculated by the Hartree Fock Bogolyubov (HFB) technique plus combinatorial deformations. A global scaling factor N_0 is applied to match with the experimental strength values. Moreover, as explained in Ref. [47], the calculated densities do not perfectly match those measured at high excitation energy. This is mainly due to the shape transitions between the ground state and the excited states which are not properly
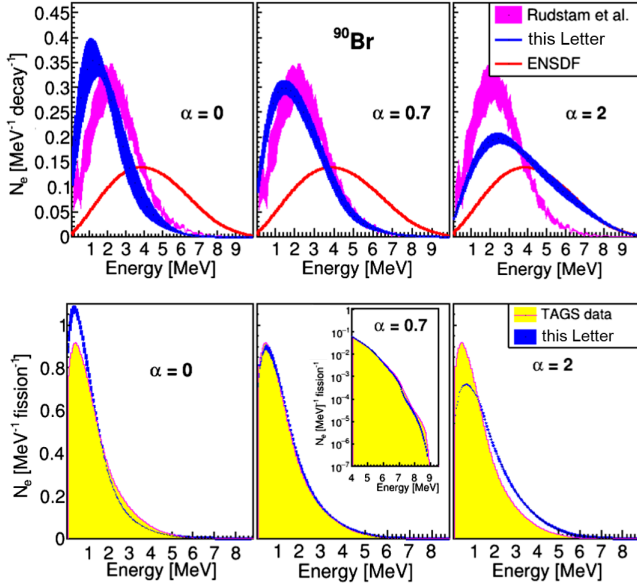
FIG. 1. Top: electron kinetic energy spectra for ^{90}Br generated with the summation model using the G-T strength model (in blue) with three α values and the ENSDF nuclear database (in red) as inputs and compared to the experimental spectrum from Ref. [48]. Bottom: cumulative electron kinetic energy spectra calculated with the summation model using the G-T strength model as input (in blue) or the TAGS experimental data (in yellow) for the same three α values. The summation was done for the 66 isotopes measured in TAGS experiments using ^{235}U fission yields for the weighting. Only the uncertainties due to the stochastic process are plotted.

taken into account in the calculations. A renormalization procedure is then needed. Following the prescriptions of Ref. [47], we have introduced a scaling function which depends on a single parameter α, for simplicity. For a given nucleus, the upper limit for the amplitudes as a function of the excitation energy (E_{exc}) is written as

$$B_{\text{GT}}^{\text{up}}(E_{\text{exc}}) = N_0 e^{-\alpha\sqrt{E_{\text{exc}}}} \rho_{\text{HFB}}(E_{\text{exc}}, Z, A) \qquad (4)$$

where α is a free parameter, common to all nuclei. Such a simple approach provides an overall good modeling of the β^- energy spectra (see top part of Fig. 1 for example) but does not allow one to reproduce each individual energy spectrum with the same α parameter.

Finally, the energy threshold between the discrete and continuous domains is determined as the energy above which the HFB level density is greater than 100 MeV^{-1}. The application of such criteria defines a threshold in the 2–3 MeV range depending on the nuclei.

The uncertainties on the energy spectra, introduced by the stochastic nature of the strength model, are calculated by running the summation model 100 times. At each iteration, a new strength function is generated for each isotope, and the intensities of the transitions are calculated using Eq. (2).

The strength model was first validated by comparing the electron energy spectra calculated with our summation method with existing measured energy spectra from Rudstam *et al.* [48]. An example is shown in Fig. 1 (top) for ^{90}Br, a large Q_β isotope with a major contribution from missing transitions. Three values of α are plotted, defining a range of physical meaning for the model. The improvement of the G-T strength model over ENSDF inputs is clearly visible. The free parameter α is used to adjust the induced correction for an optimal agreement between our prediction and the experimental spectrum, here obtained for $\alpha \sim 0.7$. This value allows a reasonable overall agreement with most of the measured spectra and is within the range of corrections to be applied on the HFB calculations provided in the RIPL3 database.

The model was also validated by comparing the cumulative energy spectra for electrons calculated for the nuclei measured in TAGS experiments, using the model or TAGS data as inputs (see Fig. 1 bottom). The best agreement is also observed for $\alpha \sim 0.7$. Because of the dominant contribution of ^{92}Rb in this region, the high energy part of the spectrum is not well reproduced. This isotope is a particular case with an almost unique transition to the ground state that our model is not able to capture perfectly: the intensity of the transition to the ground state is reduced by about 20% in our model compared with the measured TAGS data. The same agreement is observed for $\alpha \sim 0.7$ when comparing with the cumulative energy spectra for antineutrinos using TAGS data as input.

The electron and antineutrino cumulative energy spectra were calculated for ^{235}U, ^{239}Pu, and ^{241}Pu fissioning systems (data are available in the Supplemental Material [49] for three values of α around 0.7) and compared with the HM model.

Figure 2 shows the correlations, when varying α, between the number of electrons per fission, integrated over the HM range, and the average IBD cross section defined by

$$\langle\sigma_{\text{IBD}}\rangle = \int_{2\text{ MeV}}^{8\text{ MeV}} S_f(E_\nu)\sigma_{\text{IBD}}(E_\nu)dE_\nu \qquad (5)$$

using the IBD cross section (σ_{IBD}) from Ref. [3]. The use of this quantity rather than the number of neutrinos per fission is intended for direct comparison with the measured rates.

While a good agreement is found between HM and our model for ^{239}Pu and ^{241}Pu, the HM model for ^{235}U deviates from the trend. The range of α values favored by the HM model for ^{239}Pu and ^{241}Pu is also favored by STEREO [7] and Daya Bay [18] experiments. This leads us to the conclusion that the RAA could find its origin in the overestimation of the ^{235}U electron spectrum measured after 12 hours of irradiation [27] and used as reference for the HM model.
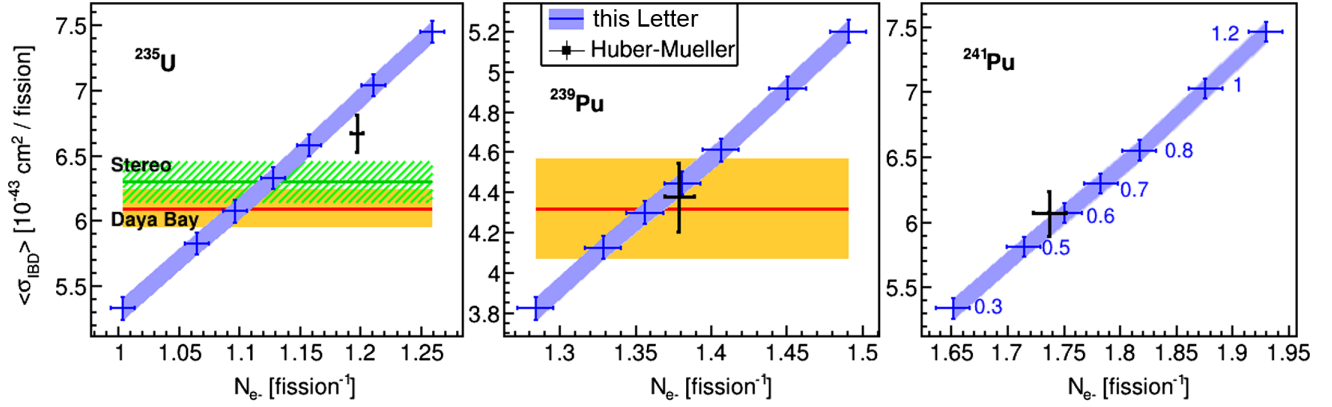
FIG. 2. Average IBD cross section per fission versus the number of electrons per fission calculated with the G-T model for the different values of α marked in the right plot and for three fissioning systems. The blue band results from the uncertainties due to the β-strength model. The uncertainties in the fission yields are lower than this band and amount to 0.4%, 0.5%, and 0.7% for ^{235}U, ^{239}Pu, and ^{241}Pu, respectively. The cross lines represent the Huber-Mueller model. Experimental results from Daya Bay [18] (orange band) and STEREO [7] (green hatch band) are also shown. Note that N_e has been integrated on the same energy range as the HM data.

Figure 3 shows the ratios to the HM model of the antineutrino and electron energy spectra calculated with our model, for three α values around 0.7. On the antineutrino side, shape discrepancies appear clearly for all fissioning isotopes. The discrepancies have the form of a bump for ^{235}U and ^{239}Pu and a global linear deviation for ^{241}Pu which does not depend too much on the α values. In the 4–6 MeV range, the excess of events around 5.5 MeV amounts to 6% for ^{235}U, 12% for ^{239}Pu, and 11% for ^{241}Pu when choosing

$\alpha = 0.7$. These values for ^{235}U and ^{239}Pu are close to the 10% deviations observed in the recent experiments [6,9–13,50,51]. As seen in the figure, the agreement with the data, from the two pure ^{235}U STEREO and PROSPECT experiments [51], is very good ($\chi^2/ndf = 17/18$) for $\alpha = 0.7$. Thus, with a simple model able to reproduce and roughly extrapolate the TAGS data, with only one free parameter, our summation model is able to describe the deviations from the HM prediction measured by recent
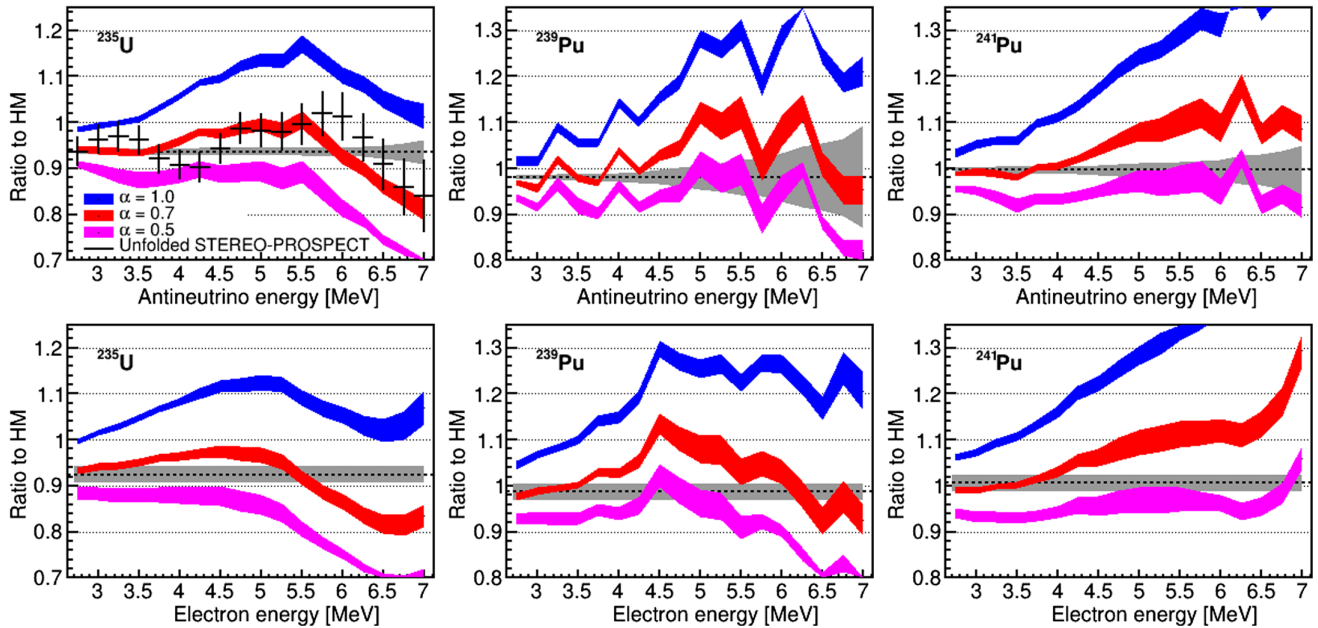

FIG. 3. Ratios of the kinetic energy spectra for ^{235}U, ^{239}Pu, and ^{241}Pu, calculated with our model for different values of α, to the Huber-Mueller model for antineutrinos (top) and electrons (bottom). The widths of the lines indicate the standard deviation of the G-T strength model due to the stochastic process. The gray band on the antineutrino side corresponds to the uncertainties in the fission yields, fully correlated between antineutrinos and electrons, while the gray band on the electron side corresponds to the systematic uncertainties in the BILL spectrometer efficiency. For comparison, the ratio to HM (scaled by a factor of 0.95 [7]) constructed with the unfolded antineutrino spectrum of Ref. [51] is added.
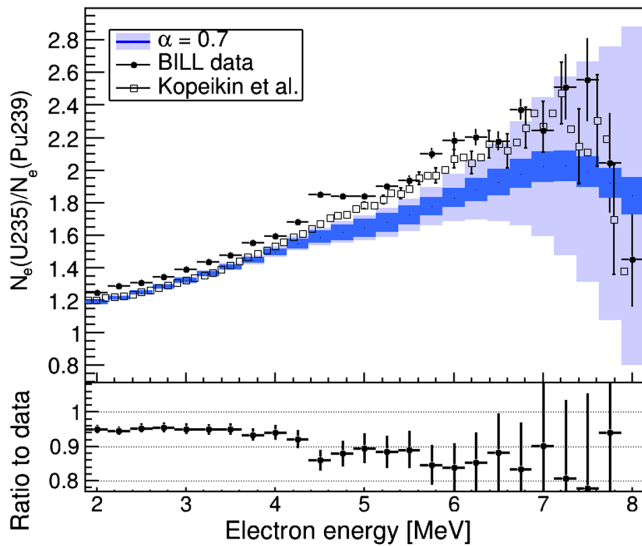
FIG. 4. Ratios of the electron kinetic energy spectra for ^{235}U and ^{239}Pu calculated with our model for $\alpha = 0.7$ and compared to experimental BILL data [27,28] (top plot). The light blue band corresponds to the total uncertainty, including fission yield uncertainties, and the dark blue band shows the uncertainty of the G-T model only. For comparison, the data from Kopeikin *et al.* [20] are added. The bottom plot is the double ratio to BILL data. All the uncertainties are propagated.

antineutrino experiments. This conclusion is valid even if α values are randomly drawn for each nucleus instead of using a common value.

All the distortions predicted on the antineutrino side are also expected on the electron side, with more or less the same amplitudes. Part of them are contained in the systematic uncertainties of the BILL spectrometer efficiency determined from the dispersion of the (n, e^-) calibration reactions, but not all.

As shown in Fig. 4, no further distortions are introduced on the ^{235}U:^{239}Pu ratio. Our model shows good agreement with the Kopeikin *et al.* measurement [20] confirming the ~5% discrepancy below 4 MeV. This result is valid even when reasonably varying the α parameter. Above 4 MeV, small deviations occur, but uncertainties are larger in this region both in the experimental data and in the model.

We therefore suspect that the anomalous feature could be attributed to a shape bias in the β^- energy spectra measured at ILL. Note that the effect of spectral changes upon the introduction of first-forbidden transitions against a treatment with allowed transitions was studied in Ref. [26]. Only the antineutrino spectrum shows significant deviations of about 5% in the [5–6] MeV range whereas it is limited for electrons. Therefore, introducing first-forbidden transitions in our model would probably reinforce the deviation to HM on the antineutrino side, without affecting the electron side. This would favor another value of α, between 0.6 and 0.7, but would not change the conclusions of this Letter.

In summary, we have presented a phenomenological Gamow-Teller strength model able to simulate β^--decay transition intensities for fission fragments and to correct for the pandemonium effect and missing transitions in the ENSDF database. Despite the model's simplicity, the main features and divergences observed in antineutrino experiments with respect to the Huber-Mueller model can be reproduced when used in a well-elaborated summation model. This study highlights the importance of missing transitions in the modeling of fission antineutrino spectra. Using the exact correspondence between electron and antineutrino in the summation approach, we have seen that equivalent deviations are expected on the electron side. The findings of this study suggest that the reactor antineutrino anomalies may originate in a norm bias for the ^{235}U spectrum measured after 12 hours of irradiation and a shape bias for all measured electron spectra. Although these conclusions are supported by independent measurements, the origin of these biases is still unclear at this stage. Biases on the neutron cross sections used to normalize the β^- spectra could cover part of the RAA [52], and part of the shape anomaly could be included in the envelope of systematic uncertainties of the BILL spectrometer efficiency. This Letter confirms the growing need to improve the accuracy of fission β^- spectra, both experimentally and theoretically, especially for precision neutrino physics at reactors.

[*]alain.letourneau@cea.fr

[†]Present address: Technical University of Munich, James-FranckStrasse 1, Garching, 85748, Germany.

[1] P. Huber, Phys. Rev. C **84**, 024617 (2011); **85**, 029901(E) (2012).

[2] T. A. Mueller, D. Lhuillier, M. Fallot, A. Letourneau, S. Cormon, M. Fechner, L. Giot, T. Lasserre, J. Martino, G. Mention, A. Porta, and F. Yermia, Phys. Rev. C **83**, 054615 (2011).

[3] G. Mention, M. Fechner, T. Lasserre, T. A. Mueller, D. Lhuillier, M. Cribier, and A. Letourneau, Phys. Rev. D **83**, 073006 (2011).

[4] D. Adey *et al.* (Daya Bay Collaboration), Phys. Rev. D **100**, 052004 (2019).

[5] G. Bak *et al.* (RENO Collaboration), Phys. Rev. Lett. **122**, 232501 (2019).

[6] Y. Abe *et al.* (Double Chooz Collaboration), J. High Energy Phys. 10 (2014) 086; 02 (2015) 74.

[7] H. Almazán *et al.* (STEREO Collaboration), Phys. Rev. Lett. **125**, 201801 (2020).

[8] H. de Kerret *et al.* (Double Chooz Collaboration), Nat. Phys. **16**, 558 (2019).

[9] F. P. An *et al.* (Daya Bay Collaboration), Phys. Rev. Lett. **116**, 061801 (2016); **118**, 099902(E) (2017); Chin. Phys. C **41**, 013002 (2017).

[10] S.-H. Seo *et al.* (RENO Collaboration), AIP Conf. Proc. **1666**, 080002 (2015).

[11] Y. J. Ko *et al.* (NEOS Collaboration), Phys. Rev. Lett. **118,** 121802 (2017).

[12] H. Almazán *et al.* (STEREO Collaboration), J. Phys. G **48,** 075107 (2021).

[13] J. Ashenfelter *et al.* (PROSPECT Collaboration), Phys. Rev. Lett. **122,** 251801 (2019).

[14] I. Alekseev *et al.* (DANSS Collaboration), Phys. Lett. B **787,** 56 (2018); I. Machikhiliyan, Phys. Part. Nuclei **53,** 546 (2022).

[15] H. Almazán *et al.* (STEREO Collaboration), Phys. Rev. D **102,** 052002 (2020).

[16] M. Andriamirado *et al.* (PROSPECT Collaboration), Phys. Rev. D **103,** 032001 (2021).

[17] M. Aker *et al.* (KATRIN Collaboration), Phys. Rev. D **105,** 072004 (2022).

[18] F. P. An *et al.* (Daya Bay Collaboration), Phys. Rev. Lett. **118,** 251801 (2017).

[19] G. Bak *et al.* (RENO Collaboration), Phys. Rev. Lett. **122,** 232501 (2019).

[20] V. Kopeikin, M. Skorokhvatov, and O. Titov, Phys. Rev. D **104,** L071301 (2021); V. Kopeikin, Yu. N. Panin, and A. A. Sabelnikov, Phys. At. Nucl. **84,** 1 (2021).

[21] D. A. Dwyer and T. J. Langford, Phys. Rev. Lett. **114,** 012502 (2015).

[22] D.-L. Fang and B. A. Brown, Phys. Rev. C **91,** 025503 (2015).

[23] A. C. Hayes, J. L. Friar, G. T. Garvey, D. Ibeling, G. Jungman, T. Kawano, and R. W. Mills, Phys. Rev. D **92,** 033015 (2015).

[24] A. A. Sonzogni, E. A. McCutchan, T. D. Johnson, and P. Dimitriou, Phys. Rev. Lett. **116,** 132502 (2016).

[25] A. A. Sonzogni, E. A. McCutchan, and A. C. Hayes, Phys. Rev. Lett. **119,** 112501 (2017).

[26] L. Hayen, J. Kostensalo, N. Severijns, and J. Suhonen, Phys. Rev. C **99,** 031301(R) (2019).

[27] W. G. K. Schreckenbach, G. Colvin, and F. von Feilitzsch, Phys. Lett. **160B,** 325 (1985).

[28] F. von Feilitzsch, A. Hahn, and K. Schreckenbach, Phys. Lett. **118B,** 162 (1982).

[29] A. Hahn, K. Schreckenbach, W. Gelletly, F. von Feilitzsch, G. Colvin, and B. Krusche, Phys. Lett. B **218,** 365 (1989).

[30] FISPACT, https://fispact.ukaea.uk/.

[31] Joint Evaluated Fission File 3.3, https://www.oecd-nea.org/dbdata/jeff/jeff33/index.html.

[32] E. F. Matthews, L. A. Bernstein, and W. Younes, Atomic Data and Nucl. Data Tables **140,** 101441 (2021).

[33] L. Perisse, Ph.D. thesis, Modeling of reactor antineutrino spectra, Université Paris-Saclay, 2021, https://tel.archives-ouvertes.fr/tel-03538198.

[34] F. G. Kondev, M. Wang, W. J. Huang, S. Naimi, and G. Audi, Chin. Phys. C **45,** 030001 (2021).

[35] M. Fallot *et al.*, Phys. Rev. Lett. **109,** 202504 (2012).

[36] M. Estienne *et al.*, Phys. Rev. Lett. **123,** 022502 (2019).

[37] ENSDF https://www.nndc.bnl.gov/ensdf/, the 2020 beta-decay data were used.

[38] J. C. Hardy, L. C. Carraz, B. Jonson, and P. G. Hansen, Phys. Lett. **71B,** 307 (1977).

[39] R. C. Greenwood, R. G. Helmer, M. H. Putnam, and K. D. Watts, Nucl. Instrum. Methods Phys. Res., Sect. A **390,** 95 (1997).

[40] A.-A. Zakari-Issoufou, M. Fallot, A. Porta *et al.*, Phys. Rev. Lett. **115,** 102503 (2015).

[41] S. Rice *et al.*, Phys. Rev. C **96,** 014320 (2017).

[42] V. Guadilla *et al.*, Phys. Rev. C **96,** 014319 (2017).

[43] V. Guadilla *et al.*, Phys. Rev. Lett. **122,** 042502 (2019).

[44] D. Jordan *et al.*, Phys. Rev. C **87,** 044318 (2013).

[45] V. Savu, Ph.D. thesis, Reactor neutrino studies: STEREO and NUCLEUS experiments, Université Paris-Saclay, 2021, https://tel.archives-ouvertes.fr/tel-03563659.

[46] RIPL3, https://www-nds.iaea.org/RIPL-3/.

[47] S. Goriely, S. Hilaire, and A. J. Koning, Phys. Rev. C **78,** 064307 (2008).

[48] G. Rudstam, P. I. Johansson, O. Tengblad, P. Aagaard, and J. Eriksen, At. Data Nucl. Data Tables **45,** 239 (1990).

[49] See Supplemental Material at http://link.aps.org/supplemental/10.1103/PhysRevLett.130.021801 to get the electron and antineutrino kinetic energy spectra for ^{235}U, ^{239}Pu and ^{241}Pu.

[50] D. Adey *et al.*, Phys. Rev. Lett. **123,** 111801 (2019); F. P. An *et al.* (Daya Bay and PROSPECT Collaborations), Phys. Rev. Lett. **128,** 081801 (2022).

[51] H. Almazán *et al.* (PROSPECT Collaboration and STEREO Collaboration), Phys. Rev. Lett. **128,** 081802 (2022).

[52] A. Onillon and A. Letourneau, *Applied Antineutrino Physics 2018 Proceedings*, https://arxiv.org/pdf/1911.06834.pdf.